Computing Black Scholes with uncertain volatility - a Bi-Fidelity approach

Kathrin Hellmuth *, Christian Klingenberg †

Abstract. We consider the Black Scholes equation with the volatility assumed to depend on a finite number of independent random variables. The aim is to quantify the effect of this uncertainty when computing the price of derivatives. Our underlying method is the generalized Polynomial Chaos (gPC) method in order to numerically compute the uncertainty of the solution by the stochastic Galerkin approach and a finite difference method. We present an efficient numerical variation of this method for solving this, which is based on a Bi-Fidelity technique. This is illustrated with numerical examples.

Key words. numerical finance, Black Scholes equation, Uncertainty Quantification, uncertain volatility, polynomial chaos, Bi-Fidelity method

AMS subject classifications. 65N35, 65N75, 91G60, 91G80

*Dept. of Mathematics, Würzburg University, Emil Fischer Str. 40, 97074 Würzburg, Germany, email: kathrin.hellmuth@t-online.de

†Dept. of Mathematics, Würzburg University, Emil Fischer Str. 40, 97074 Würzburg, Germany, email: klingen@mathematik.uni-wuerzburg.de

1. Introduction.

In modern financial markets, traders can choose from a large variety of financial derivatives. This term denotes financial instruments that have a value determined so called underlying variables or assets such as stocks, the oil price or the weather. Originally, derivatives were invented to reduce the risk of uncertain prices, especially in agricultural markets where one could have long periods between sowing and harvest, see e.g. [26] Chapter 1 or [4] Chapter I.

As the derivative market increased, also the need for a pricing formula for derivatives grew in the 20th century. A breakthrough was made by Black, Scholes [1] and Merton [14] in 1973 when they contemporaneously formulated a model allowing the evaluation of derivatives, for which they were later awarded the Nobel prize in economics. Derived from this model, the Black Scholes equation

$$\frac{\partial V(S,t)}{\partial t} + \frac{1}{2}\sigma^2 S^2 \frac{\partial^2 V(S,t)}{\partial S^2} + rS\frac{\partial V(S,t)}{\partial S} - rV(S,t) = 0, \qquad S \in (0,\infty),\, t \in [0,T], \tag{1.1}$$

explains the behaviour of the price V of the derivative by means of a partial differential equation (PDE). This derivative is allowed to depend on the time t up to maturity T and only one underlying stochastic asset, whose price is denoted by S and follows a geometric Brownian motion (e.g. a stock, an index or some commodity price). The constant r denotes the risk free rate of interest in the market and $\sigma \in \mathbb{R}$ is the so called volatility of the stochastic asset. Later, this model was extended to multiple underlying assets and adjusted for certain kinds of underlying variables like interest rates, see e.g. [3].

However, the comparison to real data soon showed that the volatility σ of one and the same stochastic asset can take values that differ more than one can explain by rounding errors etc., see e.g. [22], [23] and [8]. The most popular approaches to deal with this are to model the volatility either as local volatility, i.e. a function $\sigma(S,t)$, (see [7], [2], [5] and [9]) or as a stochastic process, compare e.g. the famous Heston model [10] or [22], [23] and [11].

Another approach is used in [15], [17] and [6]: The volatility is modelled as a one dimensional random variable $\Sigma(\omega) = \Theta(\omega)$ (in [15]) or a function of a one dimensional random variable $\Sigma(\Theta(\omega))$ (in [17] and [6]) for ω from a probability space. The resulting stochastic version of the Black Scholes equation

$$\frac{\partial V(S,t,\Theta)}{\partial t} + \frac{1}{2}\Sigma(\Theta)^2 S^2 \frac{\partial^2 V(S,t,\Theta)}{\partial S^2} + rS\frac{\partial V(S,t,\Theta)}{\partial S} - rV(S,t,\Theta) = 0 \tag{1.2}$$

is then studied by means of uncertainty quantification:
The solution V is developed in a generalized Polynomial Chaos (gPC) expansion

$$V(S,t,\Theta(\omega)) = \sum_{n=0}^{\infty} v_n(S,t) p_n(\Theta(\omega)) \tag{1.3}$$

for orthogonal polynomials p_n w.r.t. the distribution of Θ and coefficients given by the expected value $v_n(S,t) = E(V(S,t,\Theta)p_n(\Theta))$. If Θ has a density $\mu : \mathcal{D} \to \mathbb{R}$, one can alternatively calculate the coefficients by

$$v_n(S,t) = \int_{\mathcal{D}} V(S,t,x)p_n(x)\mu(x)\,dx.$$

In [15], these integrals are directly computed by a quadrature rule, where the required solutions V in the quadrature points x_j are calculated as the solutions of the deterministic Black Scholes equation 1.1 with $\sigma = x_j$. This classifies the method as a Stochastic Collocation method. In the articles of Pulch and van Emmerich [17] and Drakos [6] however, the stochastic Galerkin method is applied for computing the coefficients $v_n(S,t)$. By inserting the gPC expansion 1.3 into the stochastic Black Scholes equation, multiplying the equation by an orthogonal polynomial $p_k(\Theta)$ and applying the expected value on both sides, deterministic PDEs for the coefficients $v_n(S,t)$ are derived

$$0 = \frac{\partial v_k(S,t)}{\partial t} + \frac{1}{2}S^2 \sum_{n=0}^{\infty} \frac{\partial^2 v_n(S,t)}{\partial S^2} E\left((\Sigma(\Theta))^2 p_k(\Theta)p_n(\Theta)\right) + rS\frac{\partial v_k(S,t)}{\partial S} - rv_k(S,t). \tag{1.4}$$

After truncating of the system and the coupling term to attain a maximum index N, the system is solved numerically by the method of lines in [17] and the finite element method in [6].

In our work we extend the model used above to the volatility $\Sigma(\Theta_1,...,\Theta_L)$ depending on finitely many random variables $\Theta_1,...,\Theta_L$. This leads to the stochastic Black Scholes equation

$$\begin{aligned} 0 =& \frac{\partial V(S,t,\Theta_1,...,\Theta_L)}{\partial t} + \frac{1}{2}\Sigma^2(\Theta_1,...,\Theta_L)S^2\frac{\partial^2 V(S,t,\Theta_1,...,\Theta_L)}{\partial S^2} \\ &+ rS\frac{\partial V(S,t,\Theta_1,...,\Theta_L)}{\partial S} - rV(S,t,\Theta_1,...,\Theta_L). \end{aligned} \tag{1.5}$$

A model like this might for instance occur when the volatility is modelled as a random variable that also depends on certain stochastic factors as in [20], [21] and [19]. The solution is derived in the same way as in 1.4 and calculated numerically by a finite difference method. The computational cost for multiple similar calculations is reduced by a Bi-Fidelity technique, which can be considered as a Machine learning approach.

After introducing gPC to finitely many random variables in section 2, the stochastic Galerkin method is used to solve equation 1.5. However, computational costs can be quite high. Thus, we introduce a Bi-Fidelity numerical technique to compute this more efficiently in section 3. The paper gets rounded out with numerical results illustrating the effectiveness of this technique in section 4.

2. Deriving the system of PDEs for the gPC coefficients. Denote by $\Theta_1, ..., \Theta_L$ random variables with joint distribution function $\bar{F} : \bar{\mathcal{D}} \to \mathbb{R}$ for a multivariate domain $\bar{\mathcal{D}} \subset \mathbb{R}^L$. For a function $\bar{f} : \bar{\mathcal{D}} \to \mathbb{R}$ the following notation is used for integration with respect to (w.r.t.) $\bar{F}$:

$$\langle \bar{f} \rangle := \int_{\bar{\mathcal{D}}} \bar{f}(x_1, ..., x_L)\, d\bar{F}(x_1, ..., x_L) = E(\bar{f}(\Theta_1, ..., \Theta_L)).$$

Orthogonal polynomials w.r.t. $\bar{F}$ can be defined al follows:

Definition 2.1 (adapted from [25] Definition 8.24). *Let $\bar{F} : \bar{\mathcal{D}} \to \mathbb{R}$ be a multivariate probability distribution defined on the domain $\bar{\mathcal{D}} \subset \mathbb{R}^L$. Then a system of polynomials $\{\bar{p}_\alpha : \bar{\mathcal{D}} \to \mathbb{R} \,|\, \alpha = (\alpha_1, .., \alpha_L) \in \mathbb{N}_0^L\}$, where the polynomial $\bar{p}_\alpha(x_1, ..., x_L)$ has degree in the i-th variable $deg_{x_i}(\bar{p}_\alpha) = \alpha_i$, is called an infinite system of orthogonal polynomials w.r.t. $\bar{F}$, if for all multi indices $\alpha, \beta \in \mathbb{N}_0^L$ one has*

$$\langle \bar{p}_\alpha \bar{p}_\beta \rangle = 0 \qquad \textit{for } \alpha \neq \beta,$$
$$\langle \bar{p}_\alpha^2 \rangle =: \bar{\gamma}_\alpha > 0.$$

Existence of orthogonal polynomial systems follows from the Gram Schmidt algorithm, if for all $\alpha = (\alpha_1, ..., \alpha_L) \in \mathbb{N}_0^L$ the moments $\langle x_1^{\alpha_1} \cdot ... \cdot x_L^{\alpha_L} \rangle$ are finite. Hence, uniqueness of the orthogonal polynomials is given up to multiplication by constants. In case of independence of the Θ_i, they are in particular given by the product of the orthogonal polynomials w.r.t. the distribution of every Θ_i.

In the following, the notation $L^p_{dF}(D, H)$ denotes the space of all functions $D \to H$ that are p-times integrable w.r.t. the measure dF for some $D \subset \mathbb{R}^n$ and codomain H. If dF is not explicitly defined, the Lebesgue measure is chosen. If D and H are not defined, then D equals the domain of F and H equals $\mathbb{R}$.
It is well known, that under certain circumstances orthogonal polynomials span the space $L^2_{d\bar{F}}$. They are thus called a complete orthogonal basis of $L^2_{d\bar{F}}$.
This is for example the case, if $\bar{F}$ is absolutely continuous, has finite moments and it holds, that $(\Theta_1, ..., \Theta_L)$ realizes in a compact domain almost surely or the density of $\bar{F}$ is exponentially integrable. For details, see [18]. In case of independence of the Θ_i, the orthogonal polynomials w.r.t. $\bar{F}$ span $L^2_{d\bar{F}}$, if all orthogonal polynomial systems w.r.t. the density of Θ_i span the corresponding L^2 spaces. This is due to the tensor product representation of $L^2_{d\bar{F}}$ in case of independency of the Θ_i, see e.g. [12] Example E.10.

Assuming such circumstances to be given, the gPC expansion can be defined.

Theorem 2.2 (generalization of [25] 11.3). *Let $\Theta_1, ..., \Theta_L : \Omega \to \mathbb{R}$ be random variables with joint distribution $\bar{F}$ such that the orthogonal polynomials $(\bar{p}_\alpha)_{\alpha \in \mathbb{N}_0^L}$ w.r.t. $\bar{F}$ form a complete basis of $L^2_{d\bar{F}}$. Denote by $\mathcal{H}$ an arbitrary Hilbert space, e.g. the real numbers $\mathbb{R}$ or a space of the form $L^p(D, \mathbb{R})$, $p = 0, 1, 2$, for some domain $D \subset \mathbb{R}^n$. Then every random variable $X : \Omega \to \mathcal{H}$ with*

$$X =^d \tilde{X}(\Theta_1, ..., \Theta_L)$$

in distribution for a function $\tilde{X} \in L^2_{d\bar{F}}(\bar{\mathcal{D}}, \mathcal{H})$ can be represented in the generalized Polynomial Chaos form

$$X =^d \sum_{\alpha \in \mathbb{N}_0^L} x_\alpha \bar{p}_\alpha(\Theta_1, ..., \Theta_L) \qquad \textit{with} \qquad x_\alpha = \frac{\langle X \bar{p}_\alpha \rangle}{\langle \bar{p}_\alpha^2 \rangle} \in \mathcal{H}. \tag{2.1}$$

The proof follows in analogy to the proof for independent continuous random variables in [25] section 11.3 from the tensor product decomposition $L^2_{d\bar{F}} \otimes \mathcal{H} \cong L^2_{d\bar{F}}(\bar{\mathcal{D}}, \mathcal{H})$.

The stochastic Galerkin method is applied to the Black Scholes equation 1.5 with uncertain volatility is to transform the stochastic PDE into a system of deterministic PDEs for the gPC coefficients of the solution $V(S, t, \Theta_1, ..., \Theta_L)$.
To do so, one has to assume $\Sigma \in L^2_{d\bar{F}}$ and $V \in L^2_{d\bar{F}}(\bar{\mathcal{D}}, L^2((0,\infty) \times [0,T], \mathbb{R}))$, such that theorem 2.2 can be applied to the volatility $\Sigma(\Theta_1, ..., \Theta_L)$, the solution $V(S, t, \Theta_1, ..., \Theta_L)$ and the partial derivatives of V in S and t. In analogy to the one dimensional case in [6] and [17], inserting the gPC expansions in the Black Scholes equation 1.5 and multiplying the equation by $\bar{p}_\delta(\Theta_1, ..., \Theta_L)$ and applying the expected value, for each $\delta \in \mathbb{N}_0^L$ at a time, yields

$$0 = \frac{\partial v_\delta(S,t)}{\partial t} + \frac{1}{2} S^2 \sum_{\alpha,\beta,\gamma \in \mathbb{N}_0^L} \sigma_\alpha \sigma_\beta \frac{\partial^2 v_\gamma(S,t)}{\partial S^2} M_{\alpha\beta\gamma\delta} + rS \frac{\partial v_\delta(S,t)}{\partial S} - r v_\delta(S,t)$$

due to orthogonality of the p_α. Note that the Galerkin multiplication tensor $M_{\alpha\beta\gamma\delta} := \frac{\langle \bar{p}_\alpha \bar{p}_\beta \bar{p}_\gamma \bar{p}_\delta \rangle}{\langle \bar{p}_\delta^2 \rangle}$ exists since the integrated functions are all polynomials in L variables.
In order to solve the system, the boundary conditions and the final condition corresponding to the derivative under consideration are transformed to conditions on the gPC coefficients v_i. Usually, they are deterministic and thus appear in the coefficient $v_{(0,...,0)}$, whereas all other coefficients vanish.

After that, the gPC expansions are truncated to a finite number of terms by bounding the maximum degree $|\alpha| := \alpha_1 + ... + \alpha_L$ of the gPC expansions

$$\Sigma^K(\Theta_1, ..., \Theta_L) := \sum_{\alpha \in \mathbb{N}_0^L,\, |\alpha| \le K} \sigma_\alpha \bar{p}_\alpha(\Theta_1, ..., \Theta_L) \tag{2.2}$$

$$V^N(S, t, \Theta_1, ..., \Theta_L) := \sum_{\delta \in \mathbb{N}_0^L,\, |\delta| \le N} v_\delta^N(S,t) \bar{p}_\delta(\Theta_1, ..., \Theta_L) \tag{2.3}$$

for fixed maximum degrees $K, N \in \mathbb{N}_0$ and coefficients $v_\delta^N \in L^2((0,\infty) \times [0,T], \mathbb{R})$.
The system of equations for the truncated gPC coefficients v_δ^N, $\delta \in \mathbb{N}_0^L$ with $|\delta| \le N$, is then given by

$$0 = \frac{\partial v_\delta^N(S,t)}{\partial t} + \frac{1}{2} S^2 \sum_{\substack{\alpha,\beta,\gamma \in \mathbb{N}_0^L, \\ |\alpha|,|\beta| \le K, \\ |\gamma| \le N}} \sigma_\alpha \sigma_\beta \frac{\partial^2 v_\gamma^N(S,t)}{\partial S^2} M_{\alpha\beta\gamma\delta} + rS \frac{\partial v_\delta^N(S,t)}{\partial S} - r v_\delta^N(S,t), \tag{2.4}$$

which can be evaluated numerically.

Note, however, that convergence of the truncated stochastic Galerkin solution V^N in 2.3 to the true solution V as $N \to \infty$ is not obvious and could not be proven by now. It is a topic open to further research. However, one assumes convergence to be given in order to trust the numerical solution to represent the true solution.

3. Numerical implementation.

For demonstrative purposes, European Call options with strike price *strike* and maturity T will be considered to present the numerics used for solving the system of equations 2.4.

3.1. An explicit finite difference scheme for system 2.4.

For an easier implementation, system 2.4 is rewritten in vector form. This is done via a bijection ϕ from the set $\{0,...,|I|-1\}$ of positions in the vector to the set of multi indices $I := \{\delta \in \mathbb{N}_0^L \mid |\delta| \leq N\}$ as described in [27] section 5.2. Define $\mathbf{v} := (v^N_{\phi(0)},...,v^N_{\phi(|I|-1)})^T$, then one can represent system 2.4 by

$$\mathbf{0}_{|I|} = \frac{\partial \mathbf{v}(S,t)}{\partial t} + \frac{1}{2}S^2\mathbf{A}\frac{\partial^2 \mathbf{v}(S,t)}{\partial S^2} + rS\frac{\partial \mathbf{v}(S,t)}{\partial S} - r\mathbf{v}(S,t),$$

where the coupling matrix $\mathbf{A}$ is given by

$$\mathbf{A}[n,l] = \sum_{\substack{\alpha,\beta\in\mathbb{N}_0^L,\\ |\alpha|,|\beta|\leq K}} \sigma_\alpha\sigma_\beta M_{\alpha\beta(\phi(l))(\phi(n))}, \qquad \text{for } n,l = 0,...,|I|-1. \tag{3.1}$$

The boundary conditions and final values have to be transformed to vectors as well. For the European Call option, they are given by

$$\begin{aligned}
\mathbf{v}(S,T) &= \begin{pmatrix} (S-\mathit{strike})^+ \\ 0 \\ \vdots \\ 0 \end{pmatrix}, S \in (0,\infty), \\
\mathbf{v}(S,t) &\xrightarrow{S\to 0} \mathbf{0}_{|I|}, \qquad\qquad t \in [0,T], \qquad \text{and} \\
\frac{1}{S}\mathbf{v}(S,t) &\xrightarrow{S\to\infty} \begin{pmatrix} 1 \\ 0 \\ \vdots \\ 0 \end{pmatrix}, \qquad t \in [0,T].
\end{aligned}$$

The system has to be transformed to a finite domain. For the European Call option this can be achieved by the following transformation of variables

$$\begin{aligned}
\zeta &:= \frac{S}{S+\mathit{strike}}, \\
\tau &:= T-t, \\
\bar{\mathbf{v}}(\zeta,\tau) &:= \frac{\mathbf{v}(S,t)}{S+\mathit{strike}} = \frac{(1-\zeta)\mathbf{v}(\mathit{strike}\cdot\zeta/(1-\zeta),T-\tau)}{\mathit{strike}},
\end{aligned}$$

which can be found e.g. in [28] Chapter 2.2.5 for the deterministic Black Scholes equation. This leads to a PDE for $\bar{\mathbf{v}}$ given by:

$$\begin{aligned}
\frac{\partial \bar{\mathbf{v}}(\zeta,\tau)}{\partial \tau} &= \frac{1}{2}\zeta^2(1-\zeta)^2\mathbf{A}\frac{\partial^2 \bar{\mathbf{v}}(\zeta,\tau)}{\partial \zeta^2} + r\zeta(1-\zeta)\frac{\partial \bar{\mathbf{v}}(\zeta,\tau)}{\partial \zeta} - r(1-\zeta)\bar{\mathbf{v}}(\zeta,\tau), \\
&\qquad \zeta \in (0,1), \tau \in [0,T],
\end{aligned} \tag{3.2}$$

with boundary and initial conditions

$$\bar{\mathbf{v}}(\zeta,0) = \begin{pmatrix} (2\zeta-1)^+ \\ 0 \\ \vdots \\ 0 \end{pmatrix}, \qquad \zeta \in (0,1),$$

$$\bar{\mathbf{v}}(\zeta,\tau) \xrightarrow{\zeta\to 0} \mathbf{0}_{|I|}, \qquad \tau \in [0,T], \qquad \text{and}$$

$$\bar{\mathbf{v}}(\zeta,\tau) \xrightarrow{\zeta\to 1} \begin{pmatrix} 1 \\ 0 \\ \vdots \\ 0 \end{pmatrix}, \qquad \tau \in [0,T].$$

In order to solve the system, we choose a finite difference scheme, because it is easy to implement for practitioners. An equidistant grid

$$\zeta_m := \frac{m}{M_\zeta} = m\Delta\zeta, \quad m = 0,...,M_\zeta,$$
$$\tau^n := T\frac{n}{N_\tau} = n\Delta\tau, \quad n = 0,...,N_\tau,$$

was selected with $M_\zeta, N_\tau \in \mathbb{N}$ large enough to represent the solution in a proper way and in the right proportion to obtain a stable scheme and $\Delta\zeta := 1/M_\zeta, \Delta\tau := T/N_\tau$. The partial derivatives are approximated component wise by finite differences, as it was done for the deterministic solution in [28] Chapter 8.1.1, with

$$\text{forward differences for } \frac{\partial\bar{\mathbf{v}}}{\partial\tau}(\zeta_m,\tau^n) \approx \frac{\bar{\mathbf{v}}(\zeta_m,\tau^{n+1}) - \bar{\mathbf{v}}(\zeta_m,\tau^n)}{\Delta\tau} \quad \text{and}$$
$$\text{central differences for } \frac{\partial\bar{\mathbf{v}}}{\partial\zeta}(\zeta_m,\tau^n) \approx \frac{\bar{\mathbf{v}}(\zeta_{m+1},\tau^n) - \bar{\mathbf{v}}(\zeta_{m-1},\tau^n)}{2\Delta\zeta}$$
$$\text{and for } \frac{\partial^2\bar{\mathbf{v}}}{\partial\zeta^2}(\zeta_m,\tau^n) \approx \frac{\bar{\mathbf{v}}(\zeta_{m+1},\tau^n) - 2\bar{\mathbf{v}}(\zeta_m,\tau^n) + \bar{\mathbf{v}}(\zeta_{m-1},\tau^n)}{(\Delta\zeta)^2},$$

for $m = 1,...,M_\zeta - 1, n = 0,...,N_\tau - 1$. This yields the explicit finite difference scheme

$$\begin{aligned} \bar{\mathbf{v}}(\zeta_m,\tau^{n+1}) =& \Delta\tau\Bigg(\frac{1}{2}\zeta_m^2(1-\zeta_m)^2\mathbf{A}\frac{\bar{\mathbf{v}}(\zeta_{m+1},\tau^n) - 2\bar{\mathbf{v}}(\zeta_m,\tau^n) + \bar{\mathbf{v}}(\zeta_{m-1},\tau^n)}{(\Delta\zeta)^2} \\ & + r\zeta_m(1-\zeta_m)\frac{\bar{\mathbf{v}}(\zeta_{m+1},\tau^n) - \bar{\mathbf{v}}(\zeta_{m-1},\tau^n)}{2\Delta\zeta} - r(1-\zeta_m)\bar{\mathbf{v}}(\zeta_m,\tau^n)\Bigg) \\ & + \ \bar{\mathbf{v}}(\zeta_m,\tau^n), \end{aligned} \tag{3.3}$$

for $m = 1,...,M_\zeta - 1, n = 0,...,N_\tau - 1$ with initial value

$$\bar{\mathbf{v}}(\zeta_m,0) = \begin{pmatrix} (2\zeta_m-1)^+ \\ 0 \\ \vdots \\ 0 \end{pmatrix}, \quad m = 1,...,M_\zeta - 1.$$

The remaining values for $m \in \{0, M_\zeta\}$, i.e. $\zeta_m \in \{0,1\}$, are given by the boundary conditions $\bar{\mathbf{v}}(0,\tau^n) = \mathbf{0}_{N+1}$ and $\bar{\mathbf{v}}(1,\tau^n) = (1,0,...,0)^T$ for all n.
Consistency of the scheme can easily be verified. By the Lax-Richtmyer Equivalence theorem, see for instance [24] Theorem 1.5.1, convergence of the numerical solution is given, if M_ζ and N_τ are chosen to obtain a stable scheme 3.3 and if the system of equations 3.2 is well posed. Well posedness is in particular given for a parabolic system, i.e. when all real parts of the eigenvalues of $\mathbf{A}$ are positive.

The Galerkin multiplication tensor and thus the entries of the coupling matrix $\mathbf{A}$ can be computed by a suitable quadrature method. Gaussian quadrature was used to obtain the numerical results in section 4.

3.2. A Bi-Fidelity approach for calculating the stochastic Galerkin solution to the Black Scholes equation with random volatility.

In case of a volatility depending on $L = 2$ random variables, the SG solution truncated at maximum degree N already has $(N+1)(N+2)/2$ gPC coefficients. Thus, $(N+1)(N+2)/2$ coupled equations have to be solved to obtain the approximate SG solution. This number and with it the computational cost rapidly increase as N or L increases.
This becomes a problem especially if the SG solutions for many options shall be computed at a time. A solution to this problem is given by applying a Bi-Fidelity approach, if the same type of option (e.g. European Call options) with the same maturity T and interest rate r, but different distributions of the volatility model $\Sigma(\Theta_1, ..., \Theta_L)$ are considered. A situation like this arises for instance when comparing financial derivatives of the same type and maturity date, but with different underlying stochastic assets.

In literature, the Bi-Fidelity approach is frequently described for uncertainty quantification via Stochastic Collocation methods, see e.g. [29] and [16] for the general procedure and [13] for an application to the multi-scale Boltzmann equation. However, the same procedure can be applied to equations derived by a stochastic Galerkin method, if one takes care of the classification of the random variable.

The Bi-Fidelity method aims to approximate the desired high fidelity solution of the considered PDE, that depends on a random variable Ξ, at a certain realization z of Ξ by stored high and low fidelity solutions in some realizations of Ξ and the computationally cheaper low fidelity solution in z.
This random variable Ξ has to be assigned at first. In our case, it is not given by $(\Theta_1, ..., \Theta_L)$, since we still want our solution to be a random variable depending the Θ_i in order to explore its stochastic behaviour. Instead, we suppose the distribution of $\Sigma(\Theta_1, ..., \Theta_L)$ to change from calculation to calculation, as it would be the case for different underlying assets, without changes in the distributions of the Θ_i. By representation 2.2 of the truncated gPC expansion of Σ, a variation in the distribution of the volatility therefore means a variation in at least one of the gPC coefficients σ_α, $|\alpha| \le K$. Hence, the random variable Ξ describes volatility models of the form 2.2 by their gPC coefficients $\sigma_\alpha, |\alpha| \le K$.

Then, high and low the high fidelity models have to be defined. The high fidelity model is the one, we are actually is interested in. We chose a high resolution numerical solution to 2.4 derived by the explicit finite difference scheme 3.3

$$\begin{aligned}\bar{\mathbf{v}}(\zeta_m,\tau^{n+1}) =&\Delta\tau\Bigg(\frac{1}{2}\zeta_m^2(1-\zeta_m)^2\mathbf{A}\frac{\bar{\mathbf{v}}(\zeta_{m+1},\tau^n)-2\bar{\mathbf{v}}(\zeta_m,\tau^n)+\bar{\mathbf{v}}(\zeta_{m-1},\tau^n)}{(\Delta\zeta)^2}\\ &+r\zeta_m(1-\zeta_m)\frac{\bar{\mathbf{v}}(\zeta_{m+1},\tau^n)-\bar{\mathbf{v}}(\zeta_{m-1},\tau^n)}{2\Delta\zeta}-r(1-\zeta_m)\bar{\mathbf{v}}(\zeta_m,\tau^n)\Bigg)\\ &+\ \bar{\mathbf{v}}(\zeta_m,\tau^n),\quad \text{for } m=1,...,M_\zeta-1, n=0,...,N_\tau-1,\end{aligned}$$

with high M_ζ^H and corresponding to that, for stability, high N_τ^H. The low fidelity model, i.e. the cheaper model that is less trusted but used to define the approximation projection, is chosen to be the same numerical solution on a coarse grid with small M_ζ^L and N_τ^L.
Note, however, that N_τ^L must not be chosen too small to ensure that the scheme is stable for a large number of volatility models. The reason for this requirement will become clear at step 3.2.
Now one can proceed with the typical Bi-Fidelity algorithm as described in [16], [29] or [13].

Below, the application of the algorithm is explained, where the volatility is assumed to depend on $L=2$ random variables Θ_1,Θ_2 for a better readability. An extension to more random variables can easily be done. The truncation number $K=1$ is chosen such that the random variable Ξ represents the gPC coefficients σ_{00},σ_{10} and σ_{01}.
Since the actual computational effort lies in the calculation of the transformed system of equations 3.2 for $\bar{\mathbf{v}}=(\bar{v}^N_{\phi(0)},...,\bar{v}^N_{\phi(|I|-1)})^T$ by the scheme 3.3, the Bi-Fidelity approach is applied directly on $\bar{\mathbf{v}}$. Thus, a transformation back to the original variables $\mathbf{v}^N,S$ and t is applied only once for the Bi-Fidelity solution, reducing the computational cost. For the calculation of the scheme, initial conditions and the Galerkin multiplication tensors are stored and reused.

The following three steps describe the generation of the stored approximation data and have to be executed only once.

Step 1: At first, the co-domain of Ξ is described by finite intervals such that $\sigma_{00}\in[a_{00},b_{00}],\sigma_{10}\in[a_{10},b_{10}],\sigma_{01}\in[a_{01},b_{01}]$ if possible.
The intervals can for instance be constructed by experimentally calculating some $\sigma_{00},\sigma_{10},\sigma_{01}$ for some of the later interesting stochastic assets. Alternatively, one can think of possible values of σ_{00} inspired by experiments e.g., and choose bounds of σ_{10} and σ_{01} such that the variance of $\Sigma(\Theta_1,\Theta_2)$ is bounded. We used this approach for calculations.
After that, a large set Y of possible realizations of Ξ has to be chosen such that it is a good 'cover' of the possible values of Ξ. One can use Monte Carlo sampling or a structured grid on the co-domain of Ξ.
For every volatility model described by a $y\in Y$, the low fidelity solution $\bar{\mathbf{v}}^L(y)$ is computed, if the corresponding system of equations is parabolic and the scheme is stable.

Step 2: Since one can usually not afford to calculate the high fidelity solution in every $y \in Y$, one has to determine the $A \in \mathbb{N}$ most important points, where A denotes the number of high fidelity computations one can afford. This is achieved by choosing $z_0 := \text{argmax}_{y \in Y} d^L(\bar{\mathbf{v}}^L(y), 0))$ and

$$z_{i+1} := \underset{y \in Y}{\text{argmax}}\, d^L(\bar{\mathbf{v}}^L(y), \bar{\mathbf{V}}^L(y)^L(z_1, ..., z_i)), \qquad i = 0, ..., A-1. \tag{3.4}$$

The notation $\bar{\mathbf{V}}^L(\hat{Y}) := \text{span}(\bar{\mathbf{v}}^L(\hat{y}) \,|\, \hat{y} \in \hat{Y})$ for $\hat{Y} \subset Y$ is used and $d^L(u, V) := \inf_{v \in V} \|u - v\|^L$ is the distance of a point $v \in \bar{\mathbf{V}}^L(Y)$ to the set $V \subset \bar{\mathbf{V}}^L(y)$ induced by a norm $\|\cdot\|^L$ on $\bar{\mathbf{V}}^L(\hat{Y})$. Further details on the computation can be found in [16] algorithm 1.
This step selects the points $z_1, ..., z_A$ that span the largest subspace $\bar{\mathbf{V}}^L(z_1, ..., z_A)$ of $\bar{\mathbf{V}}^L(Y)$.

Step 3: The high fidelity solution is calculated in the thus derived points $z_1, ..., z_A$. Note that N_τ has to be chosen large enough such that the numerical scheme is stable for all volatility models z_i. Parabolicity of the system of PDEs does not have to be checked again, as it has been checked in step 1 already. The high fidelity solutions $\bar{\mathbf{v}}^H(z_i)$ and low fidelity solutions $\bar{\mathbf{v}}^L(z_i)$ are stored.

Assume now, a certain volatility model z is given and one wants to compute the Bi-Fidelity solution of the Black Scholes equation with uncertain volatility. This is done as follows:

Step 1: The low resolution numerical solution $\bar{\mathbf{v}}^L(z)$ is calculated by scheme 3.3. Note that the system of equations needs to be parabolic and the scheme has to be stable for a reasonable calculation.

Step 2: The low fidelity solution $\bar{\mathbf{v}}^L(z)$ is projected onto $\bar{\mathbf{V}}^L(z_1, ..., z_A)$ leading to the projection formula

$$\bar{v}^L(z) \approx P_{\bar{\mathbf{V}}^L(z_1,...,z_A)} \bar{\mathbf{v}}^L(z) = \sum_{k=1}^{A} c_k \bar{\mathbf{v}}^L(z_k)$$

with projection coefficients $c_k \in \mathbb{R}$ and $P_{\mathbf{V}}\mathbf{v}$ denoting the orthogonal projection of $\mathbf{v}$ onto $\mathbf{V}$. Details of the computation of the c_k can be found in [16] e.g..

Step 3: Finally, the Bi-Fidelity solution is constructed by applying the same projection law to the stored high fidelity solutions

$$\bar{\mathbf{v}}^{BF}(z) := \sum_{k=1}^{A} c_k \bar{\mathbf{v}}^H(z_k).$$

After deriving $\bar{\mathbf{v}}^{BF}$, it has to be transformed back to the original variables $\mathbf{v}$, S and t.

4. Numerical results.

This section presents numerical solutions to the Black Scholes equation with uncertain volatility. For sake of simplicity the volatility is assumed to depend on two independent random variables Θ and Δ with standard normal distribution and uniform distribution on $[-0.5, 0.5]$ respectively. The error of the Bi-Fidelity approximation is investigated and its computation time is compared to the high fidelity model. For more convenient reading, times t and the maturity T are given in days, whereas for the computations, these values were multiplied by $1/251$ to go over to years.

4.1. Results for the extended model.

The numerical solution to the truncated system of equations 2.4 for a European Call option with strike price $strike = 100$ and maturity $T = 20$ in a market with risk free rate of interest $r = 0$ is visualized in figures 1a and 1b by plotting its mean and variance.
The volatility of the underlying stochastic asset is modelled by

$$\Sigma_1(\Theta, \Delta) = 0.5 + 0.2\Theta + 0.1\sqrt{12}\Delta. \tag{4.1}$$

For the gPC expansion of the solution, the truncation number $N = 5$ was chosen, for which system 2.4 is parabolic. The numbers of grid points $M_\zeta = 200$ in ζ and $N_\tau = 319$ in τ were chosen such that the applied explicit finite difference scheme 3.3 is stable.

Contour lines were drawn at height of quarters of the maximum absolute value and the borders of the smoothing area, i.e. the area where the solution differs from its final condition $V(S,T) = (S - strike)^+$, were drawn in red. These lines will be present in each of the following surface plots. Note that the expected value surface resembles the solution of the deterministic Black Scholes equation for $\sigma = 0.5$ in figure 1c, but the smoothing area is larger.

Experiments showed that the qualitative shape of the expected value and variance is characteristic for solutions to the Black Scholes equation with random volatility 1.5 of the form $\Sigma(\Theta, \Delta) = \sigma_{00} + \sigma_{10}\Theta + \sigma_{01}\Delta$. These models lead to solutions that 'lie between' the solutions for volatility depending on Θ or Δ only with the same mean and variance of the volatility.
The higher σ_{10} is in comparison to σ_{01}, the closer the solution is to the solution for volatility depending on Θ only and the further away it is from the solution for the model depending on Δ only, vice versa. An increase in the mean σ_{00} of the volatility while keeping its variance constant was observed to enlarge the smoothing area and thus the spread of the variance, which in turn flattens it.
A rise in the variance $\sigma_{10}^2 + \sigma_{01}^2/12$ of the volatility with constant mean σ_{00}, however, seemed to scale up the variance of the SG solution by the same factor. Meanwhile, the expected value of the SG solution was marginally increased within the smoothing area.

Comparison to real market data:
The model is compared to market prices of a European Call option, whose end of day values are considered from January 7th 2019 to September 20th 2019[1]. Its underlying asset is the DAX index and the strike price and maturity are given by $strike = 10275$ and $T = 180$ days

[1]The values were obtained from *https://www.finanzen.net/*.

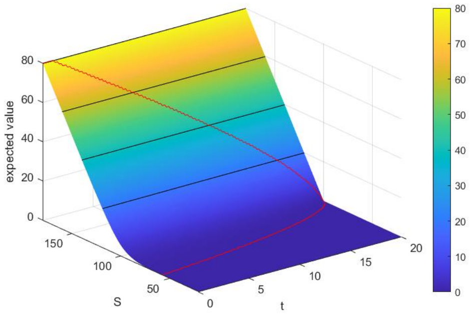

(a) Expected value surface for the stochastic solution.

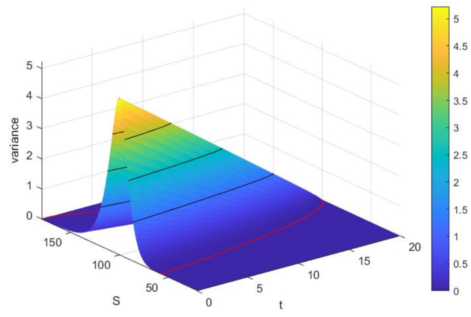

(b) Variance surface for the stochastic solution.

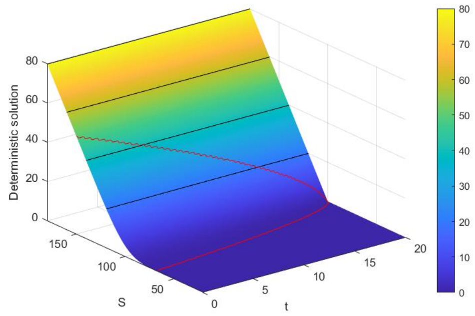

(c) Deterministic solution.

Figure 1: Solutions to the Black Scholes equation for a European call option with $T = 20, strike = 100$ and $r = 0$ for the volatility model $\Sigma_1(\Theta, \Delta) = 0.5 + 0.2\Theta + 0.1\sqrt{12}\Delta$, Θ normal distributed, in (a) and (b) and the deterministic model $\sigma = 0.5$ in (c) calculated with $K = 1, N = 5, M_\zeta = 200, N_\tau = 319$.

respectively.

A volatility model of the form $\Sigma(\Theta, \Delta) = \sigma_{00} + \sigma_{10}\Theta + \sigma_{01}\Delta$ was fitted to the data by using a maximum likelihood approach on the daily implied volatilities. This lead to the volatility model

$$\Sigma(\Theta, \Delta) = 0.2292 + 0.1126\Theta + 0.0115\Delta, \tag{4.2}$$

whose fitted density is shown in figure 2a together with a histogram density estimator. The SG solution was computed using the truncation number $N = 5$ and the numbers of grid points $M_\zeta = 200$ and $N_\tau = 678$. With these values, the numerical scheme is stable and system of equations 2.4 is parabolic.
Figure 2b shows the market prices and the expected value of the SG solution as well as the

range expected value plus/minus standard deviation and the solution to the deterministic Black Scholes equation with volatility $\sigma = E(\Sigma(\Theta, \Delta))$. A more detailed plot of those graphs for the last 55 days of the option is given in figure 2c. One observes that the expected value of the SG solution is very close to the data in these days but slightly above the data at earlier times. However, the data is always in the range expected value plus/minus standard deviation, as one would expect from stochastic theory. A comparison to the deterministic solution shows,

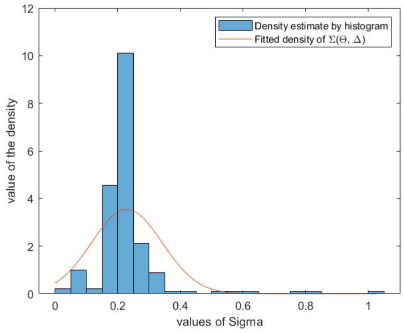

(a) Histogram density estimator and density of $\Sigma(\Theta, \Delta)$ fitted to the implied volatilities by maximum likelihood.

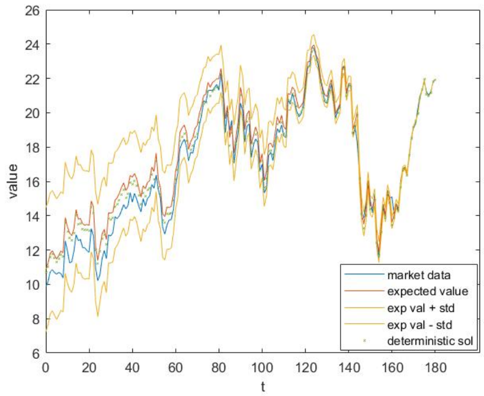

(b) Market values of the option together with the expected value of the SG solution and the range expected value plus minus standard deviation.

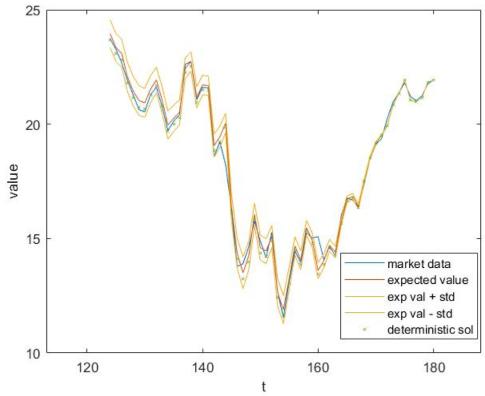

(c) Detailed look on the last 55 days.

that it also lies above the market data for early times. Recall that unlike the deterministic solution, the SG solution allows realizations to differ from the expected value within a certain range.

4.2. Comparing Bi-Fidelity solution and high fidelity solution. The Bi-Fidelity solution of the Black Scholes equation with uncertain volatility 1.5 following volatility model 4.1 for a European Call option is compared to its high fidelity solution. After that, a simulation is done to find the mean size and shape of the error in expected value and in variance between the Bi-Fidelity solution and the high fidelity solution. Finally, the computation times for high fidelity and Bi-Fidelity model are compared.

The interest rate in the market was supposed to be $r = 0$ and a maturity of $T = 23$ days was chosen. The strike price was set to $strike = 100$ and the gPC expansion of the solution was truncated after a total polynomial degree of $N = 5$ as before.

A rather coarse grid with $M_\zeta^L = 50$ and $N_\tau^L = 150$ was chosen for the low fidelity model. This N_τ^L is high enough such that the vast majority of all low fidelity computations performed in the examples explained below was stable. In case of instability, the corresponding sample point was removed from the set of low fidelity sample points. The high fidelity solution was computed on a fine grid with $M_\zeta^H + 1 = 350 + 1$ grid points in ζ direction. The number of grid points $N_\tau^H + 1 = 5853 + 1$ in τ direction was chosen such that all high resolution computations for important volatility models were stable.

The low fidelity sample points represented volatility models $\Sigma_i(\Theta, \Delta) = \sigma_{00}^{(i)} + \sigma_{10}^{(i)}\Theta + \sigma_{01}^{(i)}\Delta$ with

$$
\begin{aligned}
&\sigma_{00}^{(i)} \in \{0 < 0.05\lambda \leq 0.8 \,|\, \lambda \in \mathbb{N} \setminus \{0\}\}\,, \\
(4.3) \qquad &\sigma_{10}^{(i)} \in \left\{0.05\lambda \leq \sqrt{\sigma_{00}/2} \,|\, \lambda \in \mathbb{N}_0\right\} \quad \text{and} \\
&\sigma_{01}^{(i)} \in \left\{0.05\lambda \leq \sqrt{12(\sigma_{00}/2 - \sigma_{10}^2)} \,|\, \lambda \in \mathbb{N}_0\right\}.
\end{aligned}
$$

The coefficients were chosen such that $Var(\Sigma(\Theta, \Delta)) \leq \sigma_{00}^{(i)}/2$.
Figures 3a and 3b show the expected value surfaces of the high fidelity and the Bi-Fidelity solution for the volatility model $\Sigma(\Theta, \Delta) = 0.5 + 0.2\Theta + 0.1\sqrt{12}\Delta$. They seem to approximately coincide. To study the deviations, the absolute difference in expected values is displayed in

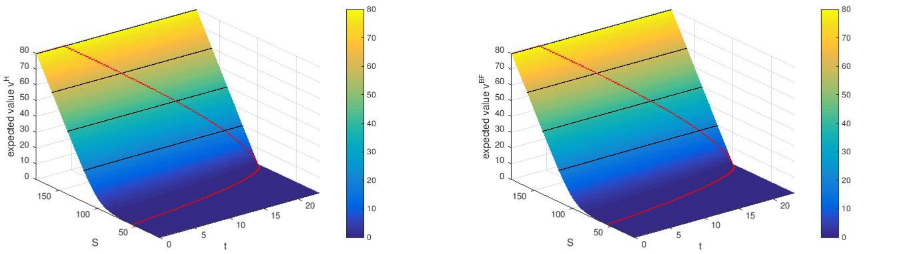

(a) Expected value surface of the high fidelity solution.

(b) Expected value of the Bi-Fidelity solution.

figures 4a close to the strike price and figure 4b for a wider range of S values. One can observe that there is some difference of size 10^{-3} within the smoothing area, but for $S \to \infty$ the difference of the two solutions seems to increase in absolute value. Figure 4c shows the difference for all values of S and t. The maximum absolute value of the absolute difference is less than 0.3 and occurs close to $S = \infty$, where the option values tends to infinity. Therefore, a difference of 0.3 in these regions means small deviation. The difference in the smoothing area of size $3 \cdot 10^{-3}$ is larger compared to the values attained in this region that are close to zero. Recall however, that the solution is multiplies by *strike* when transforming back the variables. Hence, an error of size 10^{-3} at strike 100 means an error of size $10^{-5} \cdot strike$.

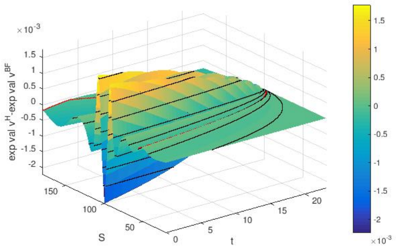

(a) close to the strike price

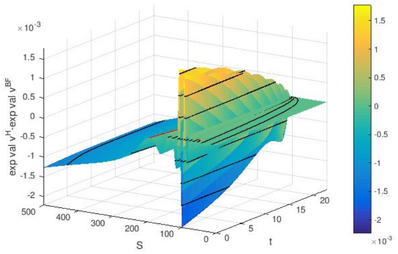

(b) for a wider range of S values

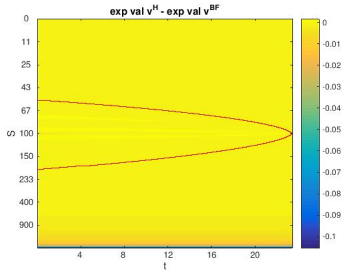

(c) for all S values

Figure 4: Absolute difference in expected value of high fidelity and Bi-Fidelity solution.

The variances of high and Bi-Fidelity solution are considered in figures 5a and 5b respectively. The high fidelity variance seems to be a little bit steeper than the Bi-Fidelity variance. We examine the absolute difference in variance as represented in figure 6a to lie in the smooth-

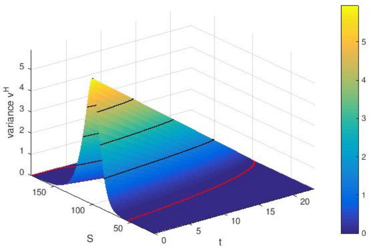

(a) Variance of the high fidelity solution.

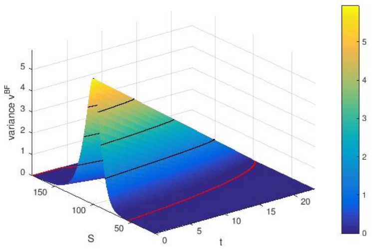

(b) Variance of the Bi-Fidelity solution.

ing area. Figure 6b showing the difference for all S and t values supports this conclusion. The error is again of size $10^{-3} = 10^{-7} \cdot strike^2$.

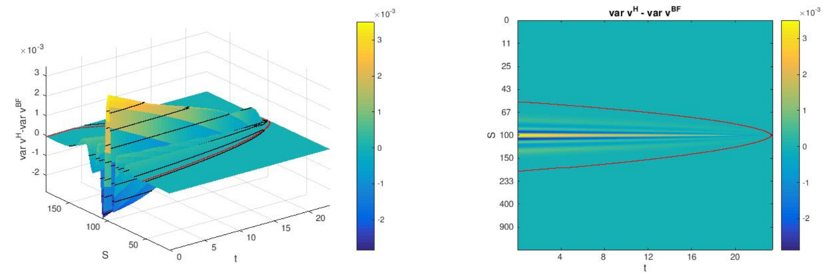

(a) close to the strike price (b) for all S values

Figure 6: Absolute difference in variance of high fidelity and Bi-Fidelity solution.

Finally, a simulation of the errors was done to obtain the mean size and shape of the Bi-Fidelity error. For this purpose, 300 volatility models of the form $\Sigma(\Theta,\Delta) = \sigma_{00}+\sigma_{10}\Theta+\sigma_{01}\Delta$ were generated randomly by obtaining the coefficients σ_{ij} as realizations of uniform random variables such that $\sigma_{00} \in [0, 0.8], \sigma_{10} \in [0, \sqrt{\sigma_{00}/2}], \sigma_{01} \in [0, \sqrt{12(\sigma_{00}/2 - \sigma_{10}^2}]$.
The mean absolute difference of the expected value of the Bi-Fidelity solution and the expected value of the high fidelity solution is represented in figure 7a close to the strike price and figure 7b for a larger range of S values. Figure 7c is a plot of the error for all S and t values. The smoothing area is not plotted, since it differs for every volatility model. The shape of the error is characterized by an oscillation of size $10^{-3} = 10^{-5} \cdot strike$ close to the strike price and a steady increase in absolute value for $S \to \infty$. The maximum absolute difference lies close to $S = \infty$ and has a size of $10^{-2} = 10^{-4} \cdot strike$, which is small in relative terms. This coincides with the error shape in figures 4a, 4b and 4c and thus seems to be characteristic for the considered Bi-Fidelity model.
The characteristic error in variances derived by the same 300 volatility models is displayed in figure 8a. It shows some oscillation close to the strike price of size $10^{-2} = 10^{-6} \cdot strike^2$, but vanishes elsewhere, as one can observe in figure 8b.

Comparing computational times
For demonstration, the above Bi-Fidelity model and the high fidelity model with the same number of grid points $M_\zeta^H = 350$ and $N_\tau^H = 5853$ were calculated in the same 300 randomly generated volatility models. Every model $\Sigma^{(i)}(\Theta,\Delta) = \sigma_{00}^{(i)} + \sigma_{10}^{(i)}\Theta + \sigma_{01}^{(i)}\Delta$ belonging to iteration $i \in \{1, ..., 300\}$ was generated such that it satisfies the same bounds on the coefficients $\sigma_{00}^{(i)} \in (0, 0.8], \sigma_{10}^{(i)} \in [0, \sqrt{\sigma_{00}/2}]$ and $\sigma_{01}^{(i)} \in [0, \sqrt{12(\sigma_{00}/2 - \sigma_{10}^2)}]$ as for the low fidelity sample points in 4.3. The $\Sigma^{(i)}$ should thus be 'covered' by the low fidelity sample points which enables a Bi-Fidelity computation. In every calculation the stability of the scheme w.r.t. the chosen time step is checked. The computation times for both models are plotted in figure 9.

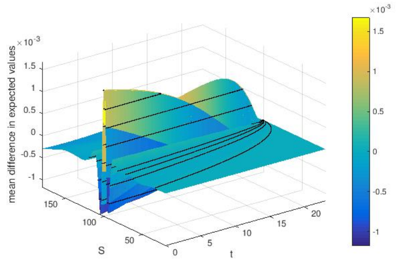

(a) close to the strike price

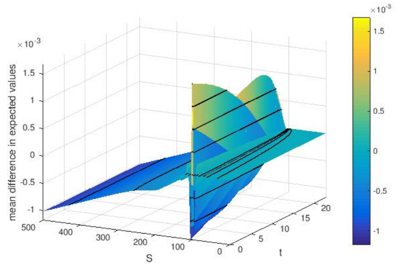

(b) for a wider range of S values

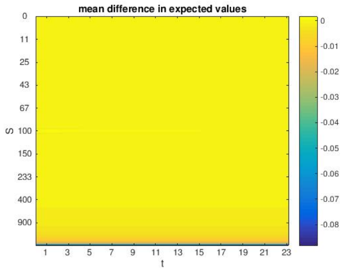

(c) for all S values

Figure 7: Mean absolute difference in expected value of high fidelity and Bi-Fidelity solution.

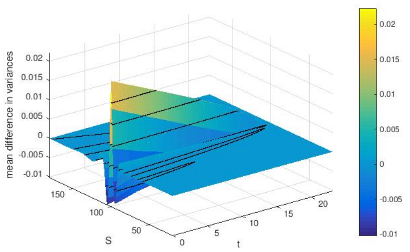

(a) within the smoothing area

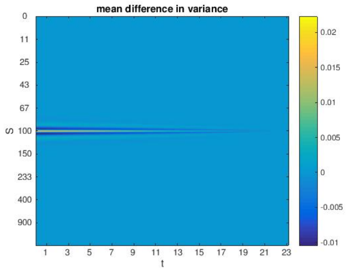

(b) for all S values

Figure 8: Mean absolute difference in variance of high fidelity and Bi-Fidelity solution.

The mean computation time for the high fidelity model is $173.99s$ whereas the Bi-Fidelity model achieved a mean computation time of $10.68s$ per volatility model. Hence, the application of the Bi-Fidelity method accelerated our computations by the factor 16.3 in mean. For finer grids, this difference should further increase. However, choosing a finer grid means introducing a larger difference in high and low fidelity model, which could introduce errors.

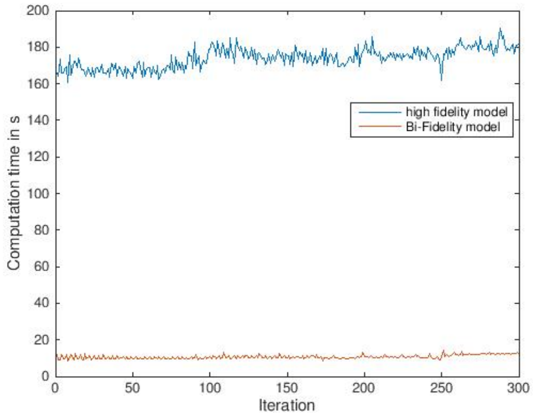

Figure 9: Computation times for the high fidelity model and the Bi-Fidelity model evaluated in the same volatility model.

5. Summary and Conclusion.

The price of a derivative was modelled by the Black Scholes equation with uncertain volatility depending on a finite number of random variables. Under certain assumptions, the random volatility and the stochastic solution can be represented by their generalized Polynomial Chaos (gPC) expansions allowing the application of the stochastic Galerkin method. The resulting deterministic system of PDEs for the gPC coefficients was truncated and solved numerically by a finite difference scheme.
Numerical examples showed that the expected value of this stochastic model fitted real market data in a similar way as a deterministic model. However, the stochastic solution allows deviations from its expected value within a certain range and it can be used for calculations of further stochastic quantities as the variance of the solution.

However, computation can become costly for a large number of random variables or a late truncation [2] due to the fast increase in the number of equations. Therefore, a machine learning technique was presented to reduce the computation cost for computing the solutions for different volatility models within the same setting (option type, maturity, interest rate, maximum polynomial degree). The so called Bi-Fidelity approach calculates the costly solution on basis of a computationally cheaper solution and some prestored costly solutions for wisely selected volatility models.
For a European Call option, the maximum absolute difference in the expected value of the Bi-Fidelity solution to desired solution was experimentally observed to be of size $10^{-5} * strike$ in mean close to the strike price and increase to size $10^{-4} * strike$ in mean for $S \to \infty$, where the expected value also tends to ∞. The maximum difference in variance attained a value of size $10^{-6} * strike^2$ in mean. Meanwhile, the mean computation time was decreased by the factor 16.3.

However, a topic that is still open to further research is the convergence of the truncated gPC expansion of the stochastic solution to the true solution as the truncation number goes to infinity. However, if convergence is assumed to hold then one could also think of solving the deterministic system of PDEs for the gPC coefficients with a different numerical technique and applying the Bi-Fidelity approach to this solution. Furthermore, one could think of applying the technique used in this paper to the Black Scholes equation with uncertain volatility and interest rate, when there are doubts concerning its true value, or to familiar equations like the Black Scholes equation for multiple assets or the bond equation.

[2] can I write that?

Acknowledgments. We would like to thank Prof. Dr. Liu Liu from the university of Hong Kong for giving us ideas and literature recommendations on the Bi-Fidelity technique. Kathrin Hellmuth was supported by a scholarship from the Hanns-Seidel-Stiftung and the Max Weber-Programm during her Bachelor and Master studies.

REFERENCES

[1] F. Black and M. Scholes, *The Pricing of Options and Corporate Liabilities*, Journal of Political Economy, 81 (1973), pp. pp. 638–654.

[2] T. Coleman, Y. Li, and A. Verma, *Reconstructing the unknown local volatility function*, The Journal of Computational Finance, 2 (1999), pp. pp. 77–102.

[3] J. C. Cox, J. Ingersoll, Jonathan E., and S. A. Ross, *A theory of the term structure of interest rates*, Econometrica, 53 (1985), pp. pp. 385–407.

[4] G. Crawford and B. Sen, *Derivatives for Decision Makers: Strategic Management Issues*, Wiley Series in Financial Engineering, Wiley, 1996.

[5] S. Crepey, *Calibration of the local volatility in a trinomial tree using Tikhonov regularization*, Inverse Problems, 19 (2002), pp. pp. 91–127.

[6] S. Drakos, *Uncertain volatility derivative model based on the polynomial chaos*, Journal of Mathematical Finance, 6 (2016), pp. pp. 55–63.

[7] B. Dupire, *Pricing with a smile*, Risk magazine, (1994), pp. pp. 18–20.

[8] M. Günther and A. Jüngel, *Finanzderivate mit MATLAB*, Vieweg + Teubner, 2nd ed., 2010.

[9] M. Hanke and E. Rösler, *Computation of Local Volatilities from Regularized Dupire Equations*, International Journal of Theoretical and Applied Finance, 8 (2005), pp. pp. 207–221.

[10] S. L. Heston, *A Closed-Form Solution for Options with Stochastic Volatility with Applications to Bond and Currency Options*, The Review of Financial Studies, 6 (1993), pp. pp. 327–343.

[11] J. C. Hull and A. White, *The Price of Options on Assets with Stochastic Volatilities*, The Journal of Finance, 42 (1987), pp. pp. 281–300.

[12] S. Janson, *Gaussian Hilbert Spaces*, Cambridge University Press, June 1997.

[13] L. Liu and X. Zhu, *A bi-fidelity method for the multiscale Boltzmann equation with random parameters*, Journal of Computational Physics, 402 (2020).

[14] R. C. Merton, *The Theory of Rational Option Pricing*, Bell Journal of Economics and Management Science, 4 (1973), pp. pp. 141–183.

[15] M. Namihira and D. A. Kopriva, *Computation of the effects of uncertainty in volatility on option pricing and hedging*, International Journal of Computer Mathematics, 89 (2012), pp. pp. 1281–1302.

[16] Narayan, Akil and Gittelson, Claude and Xiu, Dongbin, *A Stochastic Collocation Algorithm with Multifidelity Models*, SIAM Journal on Scientific Computing, 36 (2014), pp. pp. 495–521.

[17] R. Pulch and C. van Emmerich, *Polynomial chaos for simulating random volatilities*, Mathematics and Computers in Simulation, 80 (2009), pp. pp. 245–255.

[18] S. Rahman, *A polynomial chaos expansion in dependent random variables*, Journal of Mathematical Analysis and Applications, 464 (2018), pp. pp. 749–775.

[19] N. Rajput, R. Kakkar, and G. Batra, *Futures Trading and Its Impact on Volatility of Indian Stock Market*, Asian Journal of Finance and Accounting, 5 (2012).

[20] H. Reisen and J. Maltzan, *Sovereign credit ratings, emerging market risk and financial market volatility*, Intereconomics, 33 (1998), pp. pp. 73–82.

[21] S. Roy Trivedi and P. Apte, *Central Bank Intervention in USD/INR Market: Estimating Its Reaction Function and Impact on Volatility*, Asia-Pacific Financial Markets, 23 (2016), pp. pp. 263–279.

[22] M. Rubinstein, *Nonparametric Tests of Alternative Option Pricing Models Using All Reported Trades and Quotes on the 30 Most Active CBOE Option Classes from August 23, 1976 Through August 31, 1978*, The Journal of Finance, 40 (1985), pp. pp. 455–480.

[23] L. O. Scott, *Option Pricing when the Variance Changes Randomly: Theory, Estimation, and an Application*, The Journal of Financial and Quantitative Analysis, 22 (1987), pp. pp. 419–438.

[24] J. C. Strikwerda, *Finite Difference Schemes and Partial Differential Equations*, Society for Industrial

and Applied Mathematics, second ed., January 2004.

[25] T. J. Sullivan, *Introduction to Uncertainty Quantification*, vol. 63 of Texts in applied mathematics, Springer, 2015.

[26] R. Whaley, *Derivatives: Markets, Valuation, and Risk Management*, Wiley Finance, Wiley, 2007.

[27] D. Xiu, *Numerical Methods for Stochastic Computations*, Princeton University Press, 2010.

[28] Y.-l. Zhu, X. Wu, I.-L. Chern, and Z.-z. Sun, *Derivative Securities and Difference Methods*, Springer, second ed., 2013.

[29] Zhu, Xueyu and Narayan, Akil and Xiu, Dongbin, *Computational Aspects of Stochastic Collocation with Multifidelity Models*, SIAM/ASA Journal on Uncertainty Quantification, 2 (2014), pp. pp. 444–463.